LANGMUIR Article
Cite This: Langmuir 2019, 35, 16514−16520
pubs.acs.org/Langmuir

NHC-Metallosurfactants as Active Polymerization Catalysts

Adrian Donner, Bastian Trepka, Sebastian Theiss, Fabian Immler, Johanna Traber, and Sebastian Polarz*

Department of Chemistry, University of Konstanz, Universitätsstrasse 10, 78457 Konstanz, Germany

Supporting Information

ABSTRACT: Next-generation surfactants provide extended functionality apart from their amphiphilic properties. We present two novel metallosurfactants characterized by an N-heterocyclic carbene (NHC) head bearing Cu(I) and Fe(II). An innovative approach for their application in emulsion polymerizations under atom transfer radical polymerization (ATRP) conditions was developed. Thereby the complexes fulfilled the role of emulsifiers, active catalysts, and stabilization agents at once. Polymerization of methyl methacrylate (MMA) yielded stable poly(methyl methacrylate) (PMMA) colloids in water with the catalyst located at the surface of the colloids. The termination of PMMA with a bromine moiety enabled the subsequent copolymerization with styrene via macroinitiation and PMMA-polystyrene (PS) core−shell particles were obtained. Gel permeation chromatography (GPC) and selective gradient NMR experiments revealed a covalent linkage between the PMMA core and the PS shell.

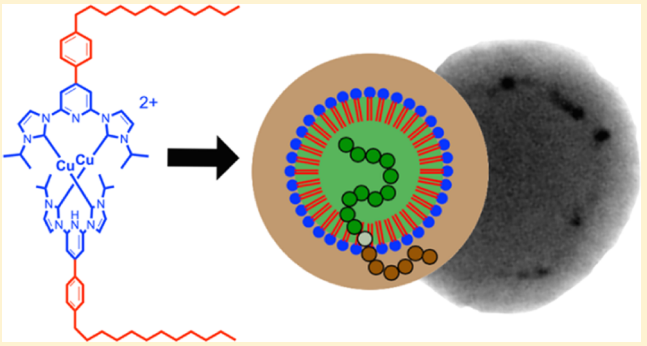

INTRODUCTION

Converting two reactants with different solvent compatibility, one hydrophilic and the other lipophilic, is a classic challenge in chemistry. This problem can be addressed by two different approaches. One approach is widely known as phase-transfer catalysis,[1,2] in which one component is moved into the unfavorable phase by coordination with auxiliaries changing its solubility. Another method is to increase the chance for a reaction by providing a large interface of the immiscible phases. This can be done by creating micelles or emulsion droplets. The current state in the associated field "micellar catalysis" was described in excellent review articles from Scarso et al. in 2015 and Lipshutz et al. in 2018.[3,4] The situation becomes even more intricate, as soon as the catalysts itself is not soluble in the desired medium. Many molecular catalysts are soluble in apolar solvents due to bulky, organic ligands coordinating to the metal. The application of those compounds in polar media, ultimately water, requires extra efforts. Here, we recommend the review published by Bhattacharya in 2009.[5] However, a remaining challenge is the compatibility of the catalytically active species with two solvents of opposing miscibility at the same time. Therefore, it would be desirable, if the surfactant itself plays a more active role during catalysis.

Surfactants are functional compounds containing hydrophilic and hydrophobic parts attached to each other in one molecule. They allow the generation of structures with a high interfacial area and are used for multiple technologies in industry and society. Next-generation surfactants provide a broader spectrum of properties beyond amphiphilicity,[6−8] and the preparation of metallosurfactants represents an elegant way to introduce such properties.[9,10] Mingotaud et al. have presented a Hoveyda's type catalyst comprising a perfluorinated C_9-chain attached to Ru via a carboxylate group in 2008.[11] Some impressive examples exist on pincer complexes with the amphiphilic design used for C−C cross-coupling reaction. For instance, Uozumi et al. prepared Palladium−NCN pincer complexes with one side modified by two alkyl chains as hydrophobic moieties and (on the other side) two oligo glycol chains for water solubility. In several publications, the authors show that the product selectivity in the Miyaura−Michael reaction can be improved in comparison to using conventional, nonamphiphilic catalysts.[12−16] N-Heterocyclic carbenes (NHCs) represent a class of ligands that are nowadays widely used in catalysis due to their robustness against thermal and oxidative stress compared to other ligands such as phosphanes.[17] Additionally, NHC ligands can easily be synthesized with a broad range of introducible additional functions.[18] Recently, we have presented surfactants containing Pd^{2+} attached to an NHC head group.[19] It was also shown, the surfactants with NHC head group are capable to coordinate to metals, but functionality has been explored only for the Pd compound. It was described that the surfactant is not only active in C−C cross-coupling reactions of the Suzuki type but also the amphiphilic design proved to be advantageous for coupling hydrophobic with hydrophilic compounds.

Received: July 12, 2019
Revised: October 30, 2019
Published: November 7, 2019

Surfactants represent inevitable constituents in emulsion polymerization techniques. A particularly powerful method is the so-called atom transfer radical polymerization (ATRP) that utilizes molecular Cu(I) as the catalyst.[20] It is a tempting concept to realize surfactants that simultaneously act as the polymerization catalyst. Back in 2001, the group of Matyjaszewski has reported, among different copper catalysts, also those with long alkyl chains attached to the ligand.[20] However, the authors did not consider any amphiphilic properties at that time. The arguments for the application of an amphiphilic NHC-system in emulsion polymerization can be summarized as follows: The huge potential of NHC-systems in the field of catalysis was mentioned above. The non-amphiphilic compounds have already been used successfully in ATRP. In polymerizations, NHC systems often play the role of organocatalysts,[21] but metal−NHC systems are used only seldom. Grubbs et al.[22] and Zhang et al.[23] presented interesting reports on Fe(II)-catalysts and Demonceau et al.[24] 24 on Ru(II)-catalysts. NHC-systems offer sufficient flexibility for chemical modification, see for instance the review article by Szczepaniak et al.,[25] which allows the preparation of tailor-made molecules.

The aim of the current publication is to establish a surfactant system, which is able to fulfill the following two tasks. It acts as a novel emulsification agent for emulsion polymerization in which no additional catalyst has to be added, because the surfactants head group is the catalyst at the same time. Based on our own preliminary results[19] and the mentioned reports in the literature, the head group is characterized by an NHC system containing Cu(I) or Fe(II) (Figure 1).

EXPERIMENTAL SECTION

Synthesis. All reactions were carried out under nitrogen in a nitrogen-filled glovebox (MBraun) or using common Schlenk techniques. THF and diethyl ether were distilled from sodium/benzophenone ketyl. Dichloromethane was distilled from CaH_2. The solvents were degassed by repetitive freeze/pump/thaw cycles and stored under dry nitrogen or argon. All other reagents were commercial grade and used as received. The amphiphilic NHC precursor (**1**)[19] and $FeCl_2(thf)_{1.5}$[26] were prepared according to literature procedures.

Amphiphilic Cu(I) Catalyst (2). The amphiphilic Cu(I) catalyst was prepared via an improved procedure previously reported by us.[19] Compound **1** (100 mg, 163 μmol) was dissolved in 5 mL of dry methanol and copper(I) oxide (233 mg, 1.63 mmol, 10 equiv) was added. The mixture was heated to 60 °C for 24 h. A color change to light green was observed. The insolubles were removed via a 0.45 μm syringe filter to yield the catalyst stock solution **2** in methanol. For the NMR analysis, the solution was evaporated to dryness. The dissolution of the residue in acetone and addition of hexane yielded compound **2** as a yellow precipitate.

^{1}H-NMR (400 Mhz, $CDCl_3$): δ (ppm) = 8.20 (s, 2H), 8.09 (s, 2H), 7.87 (d, 2H), 7.34 (d, 2H), 7.18 (s, 2H), 4.98 (quint, 2H), 2.64 (t, 2H), 1.59 (d, 12H), 1.28 (m, 20H), 0.87 (t, 3H).

ESI-HRMS (pos.): m/z = 603.3358 (measured), 603.3300 (calculated) $[C_{70}H_{98}Cu_2N_{10}]^{2+}$; deviation: 9.6 ppm.

Amphiphilic Fe(II) Catalyst (3). Compound **1** (100 mg, 163 μmol) was suspended in 5 mL of dry toluene. A solution of lithium bis(trimethylsilyl)amide (1 M solution in THF, 0.33 mL, 0.33 mmol, 2 equiv) was added dropwise and the orange solution was stirred for 2 h until all the starting materials dissolved. The solvent was removed in vacuo and a dark orange solid was obtained. A portion of dry methanol (5 mL) and $Fe(thf)_{1.5}Cl_2$ (7 mg, 2 equiv) was added and the solution was stirred for 24 h at room temperature. A color change to dark purple was observed. All insoluble compounds were removed via a 0.45 μm syringe filter to yield the stock solution of the amphiphilic catalyst **3** in methanol.

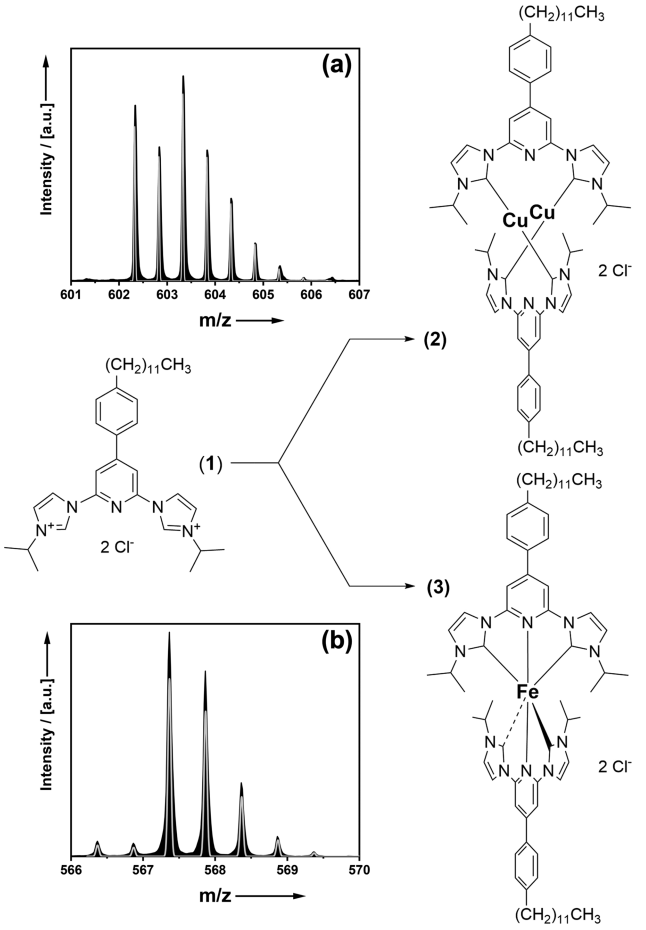

Figure 1. Synthesis scheme towards metallosurfactants with NHC head. Reaction conditions: (**2**) Cu_2O, MeOH, 60 °C, 3 days; (**3**) 1. $Li[N(SiMe_3)_2]$, Tetrahydrofuran (THF), rt, 2 h, 2. $FeCl_2(thf)_{1.5}$, MeOH, 24 h. (a) Measured electrospray ionization high-resolution mass spectrometry (ESI-HRMS) patterns of **2** (black) and calculated pattern for molecular ion $C_{70}H_{98}Cu_2N_{10}^{2+}$ (grey). (b) Measured ESI-HRMS patterns of **3** (black) and calculated pattern for molecular ion $C_{70}H_{98}FeN_{10}^{2+}$ (grey).

^{1}H-NMR (400 Mhz, $CDCl_3$): δ (ppm) = 8.85 (bs, 2H), 8.66 (bs, 2H), 8.30 (bs, 2H), 7.41 (bs, 2H), 6.92 (bs, 2H), 2.66 (quint, 2H), 2.47 (bs, 2H), 1.64 (bs, 2H), 1.27 (m, 18H), 0.87 (t, 3H), 0.73 (d, 12H). Broadening of NMR resonances and integral mismatch, typical for Fe-NHC-compounds, is observed.[27]

ESI-HRMS (pos.): m/z = 567.3647 (measured), 567.3655 (calculated) $[C_{70}H_{98}FeN_{10}]^{2+}$; deviation: 1.4 ppm.

General Procedure for the Polymerization of Methyl Methacrylate (MMA). Methylmethacrylate (1.06 mL, 1 g, 9.98 mmol) and degassed water (10 mL) were mixed and 1.25 mL of the Cu(I)/Fe(II) catalyst stock solution (40 μmol) was added. The mixture was exposed to an ultrasonic bath for 5 min and placed in a preheated oil bath (50 °C). After the final temperature was reached, the initiator ethyl α-bromoisobutyrate (6.6 μL, 8.8 mg, 45 μmol) was added. The polymerization was finished after 2 h, as no monomer was observable via gas chromatography. A liquid sample was taken for dynamic light scattering (DLS) analysis and the polymer dispersion was freeze-dried to yield the particles as a fluffy powder for electron microscopy and gel permeation chromatography (GPC) analysis.

General Procedure for the Synthesis of Poly(methyl methacrylate)/Polystyrene (PMMA/PS) Core−Shell Particles. For the synthesis of PMMA/PS core−shell particles, the total amount of monomer (9.98 mmol) was divided between MMA and PS.

DOI: 10.1021/acs.langmuir.9b02152
Langmuir 2019, 35, 16514−16520

Methylmethacrylate (0.53 mL, 0.5 g, 4.99 mmol) and degassed water (10 mL) were mixed and 1.25 mL of the Cu(I) catalyst stock solution (40 μmol) was added. The mixture was exposed to an ultrasonic bath for 5 min and placed in a preheated oil bath (50 °C). After the final temperature was reached, the initiator ethyl α-bromoisobutyrate (6.6 μL, 8.8 mg, 45 μmol) was added. The monomer conversion was monitored via gas chromatography. When no MMA was left, styrene (0.56 mL, 0.51 g, 4.99 mmol) was added and the temperature was raised to 70 °C. Raising the temperature at this point was the result of extensive screening to find the optimum reaction conditions and is consistent with temperatures used in literature for polymerization of MMA compared to styrene.[28] After no styrene was observed in gas chromatography, a liquid sample was taken for DLS analysis and the particle dispersion was freeze-dried to yield the core−shell particles as a fluffy powder for electron microscopy and GPC analysis.

Analytical Methods. Gas chromatography−mass spectrometry (GC-MS) measurements were carried out on a Thermo-Fisher Trace 1310 (FID detection, injection temperature 200 °C, temperature gradient 50−230 °C within 10 min) coupled to an ISQ QD single quadrupole mass spectrometer. ESI mass spectra were recorded on a Bruker micrOTOF focus II mass spectrometer coupled with a Dionex 3000 UHPLC (RP-C18, water/acetonitrile, 0,1% formic acid). DLS size distributions were measured on a Malvern Zetasizer Nano ZSP at 20 °C in water or methanol. Transmission electron microscopy (TEM) images were recorded either on a JEOL JEM-2200FS in scanning transmission electron microscopy (STEM) mode or on a Zeiss Libra 120. Scanning electron microscopy (SEM) images were acquired with a Zeiss Crossbeam IS40XB instrument operating at 2−5 kV. UV−vis spectra were recorded on an Agilent Cary 60 UV-Vis Spectrophotometer. For the CV measurements (THF, $^n Bu_4NPF_6$), a Wenking POS 2 potentiostat by Bank Elektronik-Intelligent Controls GmbH was used. Size exclusion chromatography (SEC) for molecular weight determination was carried out on a Polymer Laboratories PL-GPC 50 with two PLgel 5 μm MIXED-C columns in THF at 35 °C against polystyrene (PS) standards with refractive index and UV detection. High-temperature SEC was performed in 1,2,4-trichlorobenzene at 160 °C on a Polymer Laboratories 220 instrument equipped with Olexis columns with infrared and viscosity detection.

RESULTS AND DISCUSSION

Compounds **2** and **3** are obtained by the reaction of the organic ligand with Cu_2O or $FeCl_2$. Unambiguous proof for the successful synthesis of the compounds was given by NMR spectroscopy and electrospray ionization high-resolution mass spectrometry (ESI-HRMS) as shown in Figure 1.

Because the focus of the current paper is on the catalytic properties of the discussed compounds, basic surfactant characterization is kept short. Further, when working with the surfactant, care has to be taken concerning the exclosure of oxygen, because of the ease of oxidation to Cu^{II} or Fe^{III}, which was also investigated by cyclic voltammetry (CV) as shown in Supporting Information Figure S1. The latter fact also aggravated the characterization of the properties of surfactants, because most techniques like tensiometry are done in air. However, dynamic light scattering (DLS) could be performed and the occurrence of aggregates in water (≈250 nm; Figure 2) could be shown. In transmission electron micrographs, one can nicely observe the formation of vesicles with 250 nm diameter (Figure 2b). The preference for vesicle formation over micellization suggests that **2** is more similar to a lipid regarding its amphiphilic properties. DLS data for compound **3** are shown in Supporting Information Figure S2. Unfortunately, TEM was hampered by the redox activity of the surfactant, which leads to the rapid decomposition of the aggregates in the electron beam.

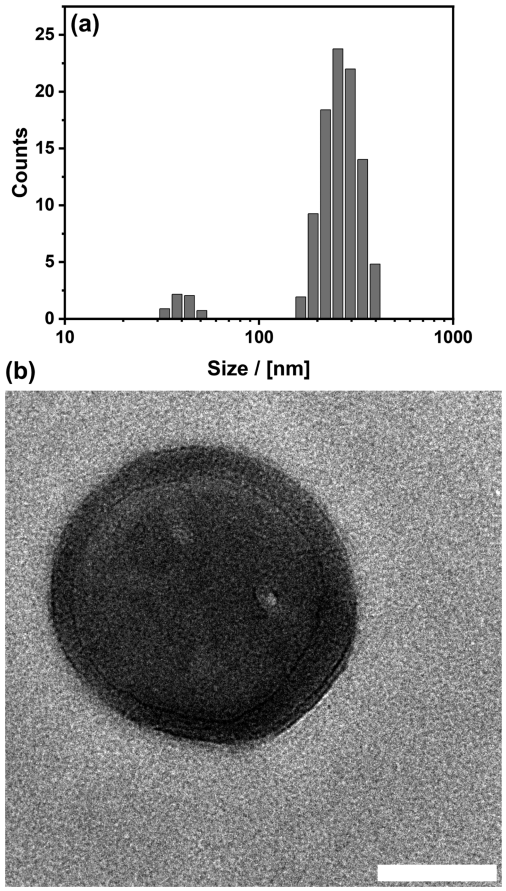

Figure 2. (a) Particle size distribution functions derived by DLS. (b) TEM micrograph (scalebar = 100 nm) of a single vesicular structure formed by the copper-containing surfactant (**2**).

Both **2** and **3** were capable of stabilizing a water/oil emulsion, as we showed exemplary for the system of interest water/methyl methacrylate (MMA) (Figure S3). We used an ATRP recipe for testing the activity of compounds **2** and **3** in catalytic emulsion polymerization. Methyl methacrylate was used as a monomer and, as often applied in ATRP, the initiator ethyl α-bromoisobutyrate ($[M]_0/[Cu]$ = 100:0.01, [I] varied from 0.01 to 0.1). Both compounds are obviously catalytically active. A stable dispersion of spherical polymer particles in water was obtained (Figure 3a).

The colloidal stability originates from a high surface charge documented by ξ-potential measurements (ξ = 50 mV). The size of particles prepared by using **3** was smaller (118 nm) compared to **2** (166 nm) according to DLS (Figure 3c) and scanning electron microscopy (SEM) (Figure 3b). The size of the particles could be adjusted (→ 98 nm → 79 nm) by lowering the MMA concentration (Figure 3c). Molecular weight (M_n = 3.1 × 10^4 to 1.05 × 10^5 Da for **2** and 3.0 × 10^5 Da for **3**) and polydispersity index of the resulting PMMA (PDI = 1.9−2.0 for **2** and 3.0 for **3**) was investigated by gel permeation chromatography (GPC) as shown in Figure 4 and Supporting Information, Figure S4. The kinetic studies of the MMA polymerization showed a linear growth of $\ln([M]_0/[M]_t)$ over time, indicating a living character of the reaction using **2** (Figure 4a). Although the PDI = 1.9−2.0 is slightly higher than expected for ideal ATRP conditions (PDI < 1.6),[29−31] it is much smaller than for a free radical process (PDI ≈ 6).[32] First of all, one has to consider that PDI values

DOI: 10.1021/acs.langmuir.9b02152
Langmuir 2019, 35, 16514−16520

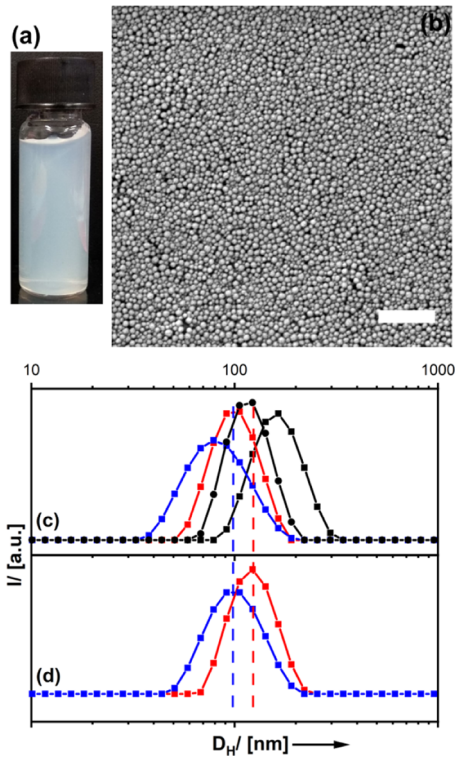

Figure 3. Photographic image of the diluted PMMA dispersion (10% of the resulting polymer latex in water) prepared using **2** as an emulsion-catalyst (a) and SEM micrograph (scale bar = 500 nm) (b). (c) DLS data of PMMA prepared by (**2**; squares) and (**3**; circles) as a catalyst. Samples prepared by lowering the monomer concentration are shown in black, red, and blue ($[M]_0/[Cat]$ = 100:0.01, 50:0.01 and 25:0.01). (d) DLS data of PMMA core particles (blue, PDI = 0.06) and core−shell particles after copolymerization with PS (red, PDI = 0.02).

for polymerization achieved by ATRP in emulsion are usually higher compared to a homogeneous process.[32] Furthermore, diffusion of the amphiphilic catalyst is hindered, because it is fixed to the interface due to its amphiphilic character.

Using **3**, the *PDI* was significantly higher, so living polymerization conditions were not achieved.[33] A potential reason is the lower redox stability of the iron compound **3** (Figure S1), which is an important prerequisite for ATRP. Although much more slowly, exposure to oxygen can also lead to the formation of Cu^{II}, which is unfavorable for ATRP. Applying the concept of reverse ATRP, i.e., the usage of the metal catalyst in its thermodynamically more stable oxidation state (e.g., Cu^{II} instead of Cu^{I}) could reduce the sensibility against oxygen.[34] However, the access to Cu^{I}/Fe^{II} NHC complexes is much more straightforward that is why we used classical ATRP conditions in this work. Because of the much better performance, we have concentrated on compound **2** instead of **3** for further experiments.

The PMMA particles were washed in several steps and were then analyzed via energy-dispersive x-ray spectroscopy (EDX). In addition to Cu and Cl from the surfactant catalyst **2**, Br could also be detected (Supporting Information Figure S5). The presence of Br can be explained by PMMA chains terminated by bromine groups. Therefore, we concluded that the particles might be able to act as a macroinitiator for further polymerizations under ATRP conditions since their surfaces were decorated by the catalyst and bromine end groups. To check, if this was the case and the catalyst was still active, we investigated next, if it was possible to attach a second monomer (styrene) to the PMMA particles in a succeeding step. The addition of styrene induced shell growth of the particles and yielded stable PMMA/PS colloids, although the surfactant remained bound to the inner core during copolymerization. The particles did not change in morphology as indicated by SEM (Supporting Information Figure S7), but their diameter increased, which could also be confirmed by DLS (Figure 3d). Because ΔD_H was of the order of 20 nm a core−shell structure with a shell thickness of 10 nm consisting of polystyrene (PS) was expected. The latter was confirmed by transmission electron microscopy (TEM) as shown in Figure 5a. Additionally, an important detail was revealed by high-angle annular dark-field (HAADF) images shown in Figure 5b. Between the inner PMMA core and the PS shell, a bright rim was observed. Since the contrast in HAADF micrographs also depends on the atomic number *Z*, the shown data indicated the presence of **2** on the surface of the PMMA spheres. This is most likely because of the high affinity of the apolar surfactants backbone to the PMMA, which occurs at a very early stage of the polymerization when the first colloids are forming. The observed bright spots can be explained by the reduction of the Cu catalyst to elemental copper by the electron beam. After the copolymerization was finished, the zeta potential ξ decreased to 25 mV (Supporting Information, Figure S6). The reduction of the electrostatic surface potential can be rationalized by two factors (Scheme 1). (a) The polystyrene shell partially shields the charge of the metal centers. (b) The number of surfactant molecules per particle is fixed, so is the number of surface

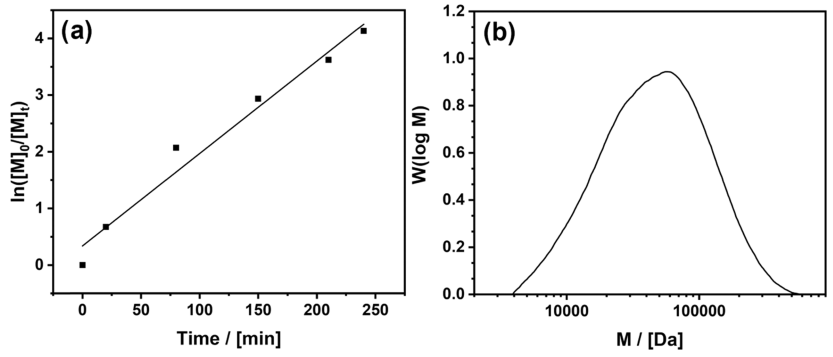

Figure 4. (a) Kinetic plot of the MMA polymerization using **2** (determined via gas chromatography using dodecane as an internal standard). (b) Molecular weight distribution of the resulting PMMA determined via GPC ($[M]_0/[Cu]/[I]$ = 100:0.01:0.01, M_n = 31 000 Da, PDI = 2.0).

DOI: 10.1021/acs.langmuir.9b02152
Langmuir 2019, 35, 16514−16520

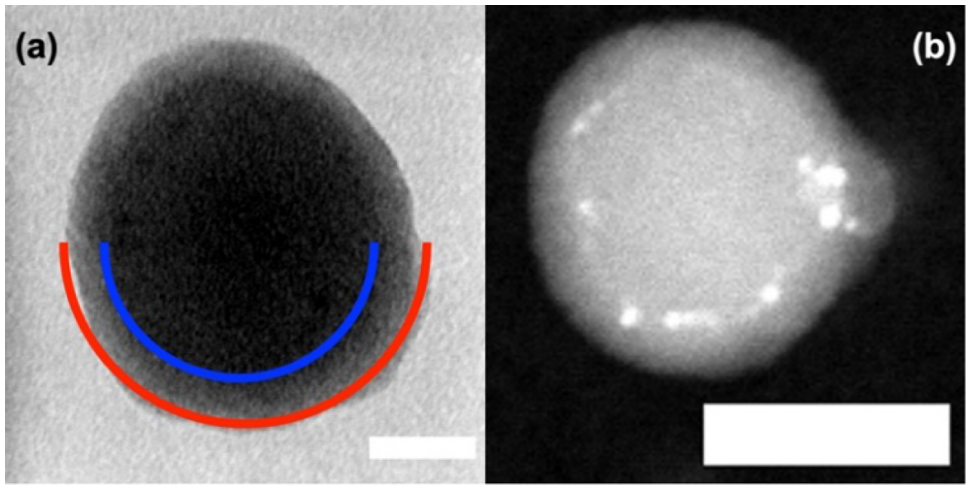

Figure 5. (a) TEM micrograph of PMMA-core (blue line) PS-shell (red line) particles prepared using (**2**) as a catalyst; scale bar = 20 nm. (b) HAADF image of the particles; scale bar = 50 nm. For an overview, see Figure S7b in Supporting Information.

Scheme 1. Formation Mechanism of the PMMA-PS Core−Shell Particles Using 2a as a Surfactant Catalyst

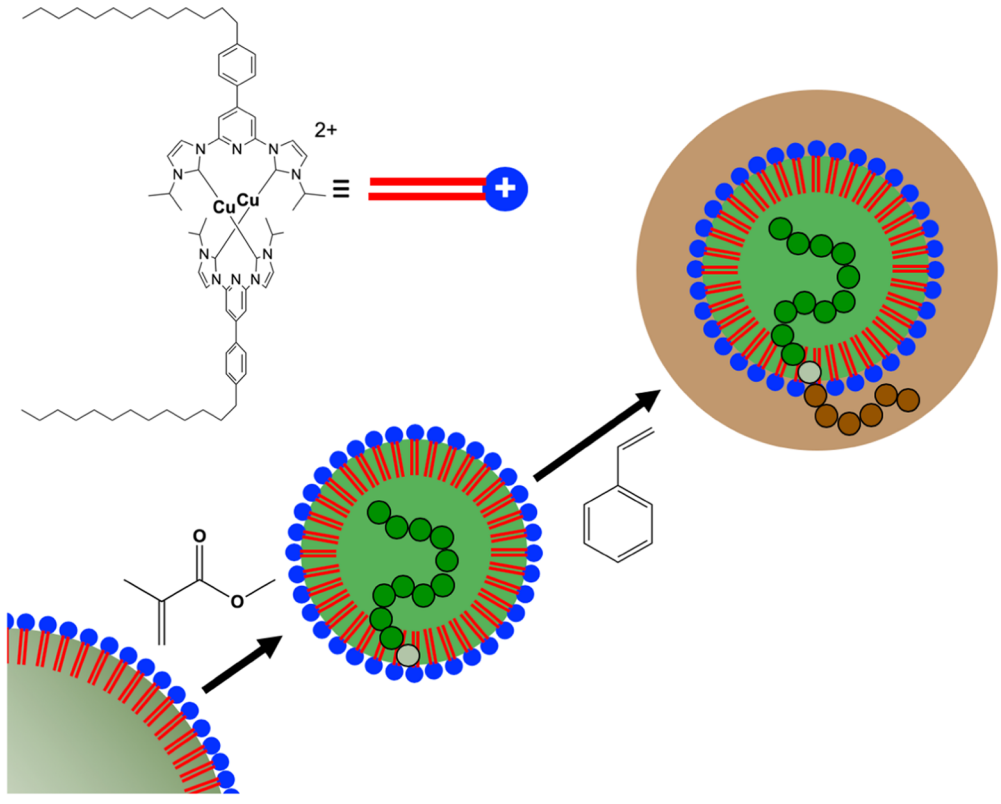

charges. But, when the particle radius increases, also its surface increases ($4\pi r^2$), and this reduces the charge density, which in turn leads to a lower surface potential. Fortunately, we found ξ = 25 mV is sufficient for colloidal stabilization. We observed that the PMMA/PS core−shell particles remain stable in dispersion over a period of one month and more.

The critical question to answer is, if the PS is just deposited on the PMMA core, or if there is the covalent linkage of the two polymer segments resulting in a PMMA/PS block copolymer in core−shell architecture. The first indications were given by GPC measurements (see also Supporting Information Figure S6). The analysis showed an increase of M_n from 3.0 × 10^4 to 6.1 × 10^4 g mol^{-1}, which matches the equimolar added amount of MMA and styrene ($M_{MMA} \approx M_{styrene}$). Furthermore, the copolymer eluted in one fraction at lower elution volumes i.e., higher molecular weight (Figure 6).

Because GPC alone does not represent unambiguous proof for the linkage of the two polymer blocks, additional techniques have to be applied. NMR spectroscopy (1D, 2D) has become a very powerful tool in polymer analytics. NMR spectra are shown in the Supporting Information Figure S9. 1D selective gradient NMR experiments enable the irradiation of distinct resonances to determine the proximity of other resonances via spin−spin coupling ("over bonds", TOCSY) or spin−lattice relaxation ("over the space", NOESY/ROESY). Covalent linkage of both polymers should generate a signal

DOI: 10.1021/acs.langmuir.9b02152
Langmuir 2019, 35, 16514−16520

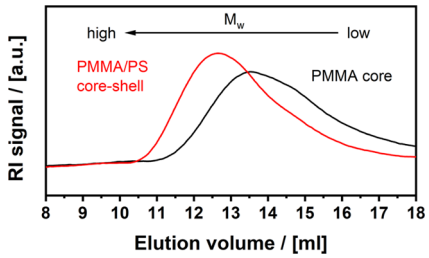

Figure 6. GPC chromatogram of the PMMA cores (black) and the PMMA/PS core–shell particles (red).

between PS and PMMA groups. Irradiation of the aromatic PS resonance at around 7 ppm revealed a strong NOE from the PS methylene signals (1.82 and 1.40 ppm), and also an answer from the PMMA methoxy and methyl protons (3.6, 1.04, and 0.85 ppm). Furthermore, 2D NOESY experiments showed, among the cross-peaks from each polymer itself, signals between the aromatic PS protons and the PMMA methoxy protons as well as from the PS methylene protons to the PMMA methoxy protons. These results show the formation of PMMA/PS core–shell particles in the form of a block copolymer. The proposed mechanism of the formation of the core–shell particles is summarized in Scheme 1.

CONCLUSIONS

In this report, we presented two NHC-metallosurfactants bearing Cu(I) or Fe(II) in their head group. Both compounds were capable of catalyzing the polymerization of MMA in emulsion under ATRP conditions. Emulsification of MMA with **2** as a surfactant leads to aggregates in water with a size of the order of 100–110 nm according to DLS and electron microscopies. Thus, the emulsion droplets (ternary system) are much smaller than the vesicles (binary system). Because according to Figure S6, the size of the PMMA-colloids remains almost constant between t = 0 and 200 min, it is most likely that the emulsion droplets formed initially represent the locus of polymerization. Furthermore, the narrow size-distribution of the polymeric particles indicates that characteristics of a microemulsion were fulfilled and there was no transport of monomers between emulsion droplets. Because the PMMA chains are terminated by bromine groups and the copper-containing surfactant is bound to the surfaces, the particles acted as macroinitiators for the copolymerization of styrene. We suppose the polymerization mechanism changes at this point as it was proven that the surfactant catalyst remains bound to the PMMA interface. The reason, why the surfactant is not able to migrate into the PS phase remains unclear at this point. A possible explanation could be that the high compatibility of the alkyl chains in **2** is much higher with the PMMA core than with the PS matrix and at the same time, a large number of aromatic rings in the head group make it compatible with the PS matrix. As a result, one can rationalize the preference of the surfactant to occupy the PMMA–PS interface.

Future possibilities of the system are of course in studying a larger variety of monomer/ polymer combinations. However, in-line with the reduction of the Zeta potential, we assume the catalytically active surfactant remains bound to the PMMA-surface of the particles. One can imagine, it is possible to remove copper at this state, resulting in NHC-covered polymer particles. Then, a different metal (e.g., Pd) can be attached to the vacant ligand sites. This would allow to grow the second shell by an entirely different mechanism, e.g., via Suzuki–Miyaura polymerization.

ASSOCIATED CONTENT

Supporting Information

The Supporting Information is available free of charge on the ACS Publications website at DOI: 10.1021/acs.langmuir.9b02152.

CV of the Cu compound (2); CV of the Fe compound (3); aggregate formation of (2) and (3) in water; TEM micrographs of aggregates; emulsification properties of (2) and (3); UV-Vis spectra of (2) and (3); TEM/SEM micrographs, GPC curves and EDX analysis of the prepared MMA particles; evolution of size and zeta potential during the polymerization; SEM/HAADF-STEM micrographs, GPC curves and NMR analysis of the prepared PMMA/PS core-shell particles (PDF)

AUTHOR INFORMATION

Corresponding Author

*E-mail: sebastian.polarz@uni-konstanz.de.

ORCID

Sebastian Polarz: 0000-0003-1651-4906

Author Contributions

The manuscript was written through the contributions of all authors. All authors have given approval to the final version of the manuscript.

Funding

The current research was funded by an ERC consolidator grant (I-SURF; project 614606).

Notes

The authors declare no competing financial interest.

ACKNOWLEDGMENTS

The authors thank the European Research Council (ERC) for funding within the project "I-SURF" and the Deutsche Forschungsgemeinschaft (DFG) for funding within the framework of the Collaborative Research Center SFB-1214 - project Z1 (Particle Analysis Center). Furthermore, the authors thank Manuel Schnitte and Florian Wimmer for GPC and Anke Friemel for NMR measurements.

REFERENCES

(1) Starks, C. M. Phase-Transfer Catalysis. 1. Heterogeneous Reactions Involving Anion Transfer by Quarternary Ammonium and Phosphonium Salts. *J. Am. Chem. Soc.* **1971**, *93*, 195–199.

(2) Ooi, T.; Maruoka, K. Recent advances in asymmetric phase-transfer catalysis. *Angew. Chem., Int. Ed.* **2007**, *46*, 4222–4266.

(3) La Sorella, G.; Strukul, G.; Scarso, A. Recent advances in catalysis in micellar media. *Green Chem.* **2015**, *17*, 644–683.

(4) Lipshutz, B. H.; Ghorai, S.; Cortes-Clerget, M. The Hydrophobic Effect Applied to Organic Synthesis: Recent Synthetic Chemistry "in Water". *Chem. - Eur. J.* **2018**, *24*, 6672–6695.

(5) Bhattacharya, S.; Kumari, N. Metallomicelles as potent catalysts for the ester hydrolysis reactions in water. *Coord. Chem. Rev.* **2009**, *253*, 2133–2149.

(6) Polarz, S.; Kunkel, M.; Donner, A.; Schlotter, M. Added-Value Surfactants. *Chem. - Eur. J.* **2018**, *24*, 18842–18856.

(7) Bijlard, A. C.; Wald, S.; Crespy, D.; Taden, A.; Wurm, F. R.; Landfester, K. Functional Colloidal Stabilization. *Adv. Mater. Interfaces* **2017**, *4*, No. 1600443.

DOI: 10.1021/acs.langmuir.9b02152
Langmuir 2019, 35, 16514–16520

(8) Brown, P.; Hatton, T. A.; Eastoe, J. Magnetic surfactants. *Curr. Opin. Colloid Interface Sci* **2015**, *20*, 140−150.
(9) Griffiths, P. C.; Fallis, I. A.; Chuenpratoom, T.; Watanesk, R. Metallosurfactants: Interfaces and micelles. *Adv. Colloid Interface Sci.* **2006**, *122*, 107−117.
(10) Kaur, R.; Mehta, S. K. Self aggregating metal surfactant complexes: Precursors for nanostructures. *Coord. Chem. Rev.* **2014**, *262*, 37−54.
(11) Mingotaud, A.-F.; Krämer, M.; Mingotaud, C. Catalytic surfactants for ring-opening metathesis polymerization and ring-closing metathesis in non-degassed micellar solutions. *J. Mol. Catal. A: Chem.* **2007**, *263*, 39−47.
(12) Hamasaka, G.; Muto, T.; Uozumi, Y. Molecular-Architecture-Based Administration of Catalysis in Water: Self-Assembly of an Amphiphilic Palladium Pincer Complex. *Angew. Chem., Int. Ed.* **2011**, *50*, 4876−4878.
(13) Hamasaka, G.; Muto, T.; Uozumi, Y. A novel amphiphilic pincer palladium complex: design, preparation and self-assembling behavior. *Dalton Trans.* **2011**, *40*, 8859−8868.
(14) Hamasaka, G.; Uozumi, Y. The Development of a Vesicular Self-assembled Amphiphilic Platinum NCN-Pincer Complex and Its Catalytic Application to Hydrosilylation of Alkenes in Water. *Chem. Lett.* **2016**, *45*, 1244−1246.
(15) Hamasaka, G.; Muto, T.; Andoh, Y.; Fujimoto, K.; Kato, K.; Takata, M.; Okazaki, S.; Uozumi, Y. Detailed Structural Analysis of a Self-Assembled Vesicular Amphiphilic NCN-Pincer Palladium Complex by Using Wide-Angle X-Ray Scattering and Molecular Dynamics Calculations. *Chem. - Eur. J.* **2017**, *23*, 1291−1298.
(16) Hamasaka, G.; Uozumi, Y. Cyclization of alkynoic acids in water in the presence of a vesicular self-assembled amphiphilic pincer palladium complex catalyst. *Chem. Commun.* **2014**, *50*, 14516−8.
(17) Kantchev, E. A. B.; O'Brien, C. J.; Organ, M. G. Palladium Complexes of N-Heterocyclic Carbenes as Catalysts for Cross-Coupling Reactions—A Synthetic Chemist's Perspective. *Angew. Chem., Int. Ed.* **2007**, *46*, 2768−2813.
(18) Peris, E. Smart N-Heterocyclic Carbene Ligands in Catalysis. *Chem. Rev.* **2018**, *118*, 9988−10031.
(19) Donner, A.; Hagedorn, K.; Mattes, L.; Drechsler, M.; Polarz, S. Hybrid Surfactants with N-Heterocyclic Carbene Heads as a Multifunctional Platform for Interfacial Catalysis. *Chem. - Eur. J.* **2017**, *23*, 18129−18133.
(20) Pintauer, T.; Matyjaszewski, K. Structural aspects of copper catalyzed atom transfer radical polymerization. *Coord. Chem. Rev.* **2005**, *249*, 1155−1184.
(21) Fèvre, M.; Pinaud, J.; Gnanou, Y.; Vignolle, J.; Taton, D. N-Heterocyclic carbenes (NHCs) as organocatalysts and structural components in metal-free polymer synthesis. *Chem. Soc. Rev.* **2013**, *42*, 2142−2172.
(22) Louie, J.; Grubbs, R. H. Highly active iron imidazolylidene catalysts for atom transfer radical polymerization. *Chem. Commun.* **2000**, *16*, 1479−1480.
(23) Chen, M.-Z.; Sun, H.-M.; Li, W.-F.; Wang, Z.-G.; Shen, Q.; Zhang, Y. Synthesis, structure of functionalized N-heterocyclic carbene complexes of Fe(II) and their catalytic activity for ring-opening polymerization of e-caprolactone. *Journal of Organometallic Chemistry* **2006**, *691* (11), 2489−2494.
(24) Delaude, L.; Delfosse, S.; Richel, A.; Demonceau, A.; Noels, A. F. Tuning of ruthenium N-heterocyclic carbene catalysts for ATRP. *Chem. Commun.* **2003**, 1526−1527.
(25) Szczepaniak, G.; Kosiński, K.; Grela, K. Towards "cleaner" olefin metathesis: tailoring the NHC ligand of second generation ruthenium catalysts to afford auxiliary traits. *Green Chem.* **2014**, *16*, 4474−4492.
(26) Kern, R. J. Tetrahydrofuran complexes of transition metal chlorides. *J. Inorg. Nucl. Chem* **1962**, *24*, 1105−1109.
(27) Anneser, M. R.; Haslinger, S.; Pöthig, A.; Cokoja, M.; Basset, J.-M.; Kühn, F. E. Synthesis and Characterization of an Iron Complex Bearing a Cyclic Tetra-N-heterocyclic Carbene Ligand: An Artifical Heme Analogue? *Inorg. Chem.* **2015**, *54*, 3797−3804.
(28) Wang, J. S.; Matyjaszewski, K. Controlled/"Living" Radical Polymerization. Halogen Atom Transfer Radical Polymerization Promoted by a Cu(I)/Cu(II) Redox Process. *Macromolecules* **1995**, *28*, 7901−7910.
(29) Benoit, D.; Chaplinski, V.; Braslau, R.; Hawker, C. J. Development of a universal alkoxyamine for "living" free radical polymerizations. *J. Am. Chem. Soc.* **1999**, *121*, 3904−3920.
(30) Matyjaszewski, K.; Shipp, D. A.; Wang, J. L.; Grimaud, T.; Patten, T. E. Utilizing halide exchange to improve control of atom transfer radical polymerization. *Macromolecules* **1998**, *31*, 6836−6840.
(31) Wang, X. S.; Armes, S. P. Facile atom transfer radical polymerization of methoxy-capped oligo(ethylene glycol) methacrylate in aqueous media at ambient temperature. *Macromolecules* **2000**, *33*, 6640−6647.
(32) Min, K.; Matyjaszewski, K. Atom Transfer Radical Polymerization in Microemulsion. *Macromolecules* **2005**, *38*, 8131−8134.
(33) Percec, V.; Guliashvili, T.; Ladislaw, J. S.; Wistrand, A.; Stjerndahl, A.; Sienkowska, M. J.; Monteiro, M. J.; Sahoo, S. Ultrafast synthesis of ultrahigh molar mass polymers by metal-catalyzed living radical polymerization of acrylates, methacrylates, and vinyl chloride mediated by SET at 25 degrees C. *J. Am. Chem. Soc.* **2006**, *128*, 14156−14165.
(34) Wang, J.-S.; Matyjaszewski, K. "Living"/Controlled Radical Polymerization. Transition-Metal-Catalyzed Atom Transfer Radical Polymerization in the Presence of a Conventional Radical Initiator. *Macromolecules* **1995**, *28*, 7572−7573.

DOI: 10.1021/acs.langmuir.9b02152
Langmuir 2019, 35, 16514−16520